IRIS AperTO

UNIVERSITÀ DEGLI STUDI DI TORINO

AperTO - Archivio Istituzionale Open Access dell'Università di Torino

Wind generated rogue waves in an annular wave flume

This is a pre print version of the following article:

Original Citation:

Availability:

This version is available http://hdl.handle.net/2318/1627211 since 2017-03-03T10:12:49Z

Terms of use:

Open Access

Anyone can freely access the full text of works made available as "Open Access". Works made available under a Creative Commons license can be used according to the terms and conditions of said license. Use of all other works requires consent of the right holder (author or publisher) if not exempted from copyright protection by the applicable law.

(Article begins on next page)

26 August 2022

arXiv:1609.06958v1 [physics.flu-dyn] 22 Sep 2016

Wind generated rogue waves in an annular wave flume

A. Toffoli[1], D. Proment[2], H. Salman[2], J. Monbaliu[3], F. Frascoli[4], M. Dafilis[5], E. Stramignoni[6], R. Forza[6], M. Manfrin[6], and M. Onorato[6,7]
[1]*Department of Infrastructure Engineering, The University of Melbourne, Parkville, VIC 3010, Australia;*
[2]*School of Mathematics, University of East Anglia, Norwich Research Park, Norwich, NR4 7TJ, UK;*
[3]*K.U. Leuven, Kasteelpark Arenberg 40, 3001 Heverlee, Belgium;*
[4]*Department of Mathematics, Faculty of Science, Engineering and Technology, Swinburne University of Technology, Hawthorn, VIC 3122, Australia;*
[5]*Department of Health and Medical Sciences, Faculty of Health, Art and Design, Swinburne University of Technology, Hawthorn, VIC 3122, Australia;*
[6]*Dipartimento di Fisica, Università degli Studi di Torino, Via Pietro Giuria 1, 10125 Torino, Italy;*
[7]*INFN, Sezione di Torino, Via Pietro Giuria 1, 10125 Torino, Italy.*

(Dated: September 23, 2016)

We investigate experimentally the statistical properties of a wind-generated wave field and the spontaneous formation of rogue waves in an annular flume. Unlike many experiments on rogue waves, where waves are mechanically generated, here the wave field is forced naturally by wind as it is in the ocean. What is unique about the present experiment is that the annular geometry of the tank makes waves propagating circularly in an *unlimited-fetch* condition. Within this peculiar framework, we discuss the temporal evolution of the statistical properties of the surface elevation. We show that rogue waves and heavy-tail statistics may develop naturally during the growth of the waves just before the wave height reaches a stationary condition. Our results shed new light on the formation of rogue waves in a natural environment.

Rogue waves are rare events of exceptional height that may surge without warnings [1–4]. This peculiar phenomenon is ubiquitous. It has been observed in different contexts such as gravity and capillary waves [5–10], optical fibres [11–17], superfluid helium [18] and plasmas [19, 20]. Because of their universal and potentially detrimental nature, there is a pressing need to understand their physics in order to predict and control them.

The generating mechanisms can be disparate [21]. These include the spatio-temporal linear focussing of wave energy [22, 23], the focussing due to bathymetry and currents (see e.g. [24–26]) and the self-focussing that results from the Benjamin-Feir instability [27]. The latter is described by exact breather solutions of the nonlinear Schrödinger (NLS) equation [28], which are coherent structures that oscillate in space and/or time. Interestingly enough, breathers can also exist embedded in random waves [29]. Provided that the ratio of the dominant wave steepness to the spectral bandwidth is $O(1)$ and propagation is unidirectional, large amplitude structures can occur often enough to originate strong deviations from Gaussian statistics [6, 15, 29–31]. Therefore, breathers have been considered in various fields of physics as a plausible prototype of rogue waves.

Such solutions have been reproduced experimentally in wave tanks using prescribed boundary conditions at the wave maker [8]. Indeed, the standard form of NLS describes the nonlinear dynamics of a pre-existing (initial) wave field, which propagates without gaining or losing energy. This framework, however, is not transferable in a straightforward manner to systems driven by external forcing. The most obvious example of such a context is the ocean, where the oscillatory motion of the water surface is generated by the forcing of local wind (the resulting wave field is generally known as wind sea). Waves then grow with fetch and/or time until a quasi-stationary condition is reached, i.e. a fully developed sea [32]. Experimental work in wave tanks where waves are generated only by winds have been reported in the past, see for example Ref. [33–35]. Due to finite-length constraints of wind-wave flumes, experiments are performed in fetch-limited and statistically stationary conditions, with moderately small fetches. Under these circumstances, it has been observed that statistical properties of the surface elevation only weakly deviates from Gaussian statistics.

In the present Letter, we discuss a laboratory wind-sea experiment in an annular flume, over which a constant and quasi-homogeneous wind blows. Instead of the *fetch-limited* and time-independent settings that have characterised previous experiments in rectilinear flumes, the annular geometry impose a so-called *duration-limited* condition [36]. Our peculiar facility allows the observation of the continuous growth in time, from the initial still water surface, to the fully developed condition. We show that during the very early stages of the generation, characterised by a growth of the wave height and a downshift of the spectral peak, the statistics is close to Gaussian. Just before the wave spectrum reaches its stationary state, the maximum deviations from Gaussian statistics and formation of rogue waves are observed. Once stationarity is reached, the statistics falls back to a Gaussian regime.

The experiment was conducted in the geophysical circular wave flume at the University of Turin. The flume has an outside diameter of $5\,m$ and an inside diameter of $1\,m$ (Fig. 1a). The annular region of $2\,m$ width was filled with $0.46\ m$ of water, leaving a closed air chamber

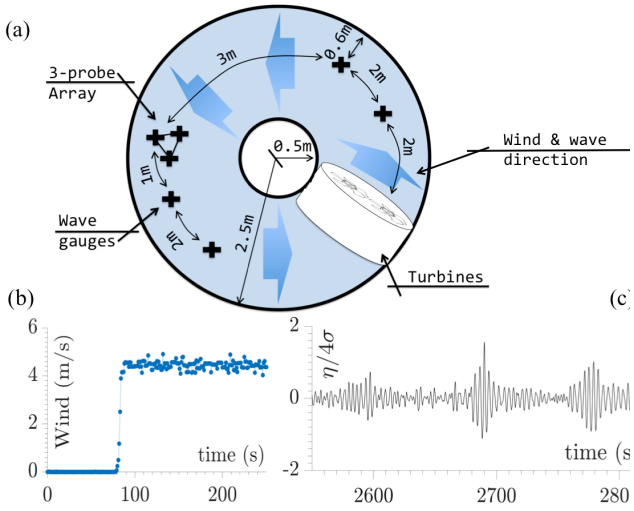

FIG. 1. Experimental set up (not in scale, panel a); examp of wind speed (panel b); and example of water surface elev tion (normalised by four times the standard deviation of tl 10-minute record), including a rogue wave with wave heig 2.7 times higher than the significant wave height (panel c).

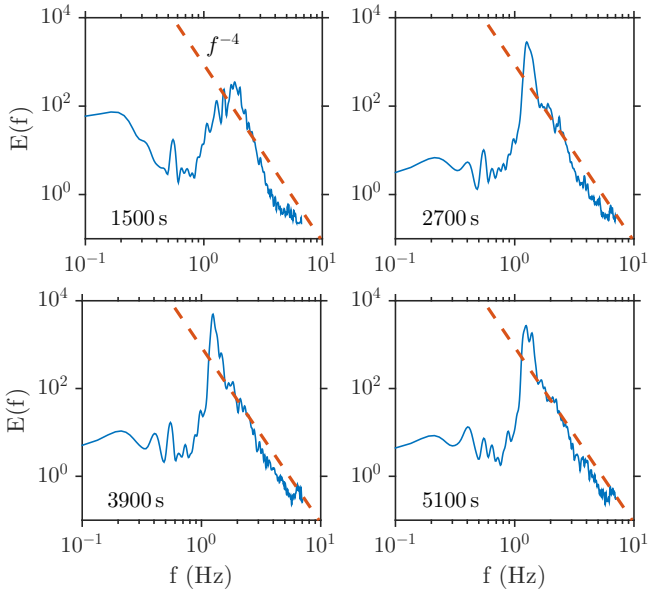

FIG. 2. Temporal evolution of the wave spectrum as a function of the intrinsic frequency. Slope corresponding to a decay at f^{-4} is shown as a dashed line.

above the water surface of approximately $0.5\,m$. Two $2.2\,KW$ industrial fans (flow rate of $9600\,m^3/h$) were then mounted in the circuit for the generation of the wind. The air flow was measured by a three-dimensional ultrasonic anemometer, which operated at a sampling rate of $20.8\,Hz$, and a hot wire, which recorded the air flow at sampling frequency of $1\,Hz$. Both instruments were deployed at about $0.3\,m$ above the still water level. The water surface was traced by a total of seven capacitance wave gauges, operating at a sampling frequency of $50\,Hz$. Four wave gauges were deployed at a distance of $2\,m$, $4\,m$, $8\,m$ and $10\,m$ from the turbines (distances are taken counter-clockwise along the arc-length). Without loss of generality, only wave data from the farthest probes (at $8\,m$ and $10\,m$ from the turbines) are discussed herein. An additional three-gauge array was installed at about $7\,m$ from the fans. The array had a shape of an equilateral triangle circumscribed in a circle of diameter of $0.2\,m$. The configuration of this array was specifically designed to measure the full directional spectrum. A high-resolution acoustic velocimeter was also used to measure water flow at a sampling frequency of $50\,Hz$. Note that the velocity field in the water comprises a wave-induced oscillatory motion and a wind-induced current.

The still water surface was the initial condition for the experiment. Fans were then turned on to produce a steady wind that reached rapidly a target speed of $4\,m/s$ (see an example of wind time series as recorded by the hot wire in Fig. 1b). Wind was kept blowing without interruptions for two hours. At regime, the air friction velocity was calculated to be $u_* = 0.21\,m/s$ and the wind-induced water flow was measured to be approximately $U = 0.07\,m/s$. The water surface elevation was monitored continuously during the entire test. Post processing was carried out on 10-minute records. The experimental test was repeated four times to ensure statistical robustness of the results.

A Fourier Transform algorithm was applied to the time series to reconstruct the distribution of the wave energy in frequency domain. For each 10-minute block, the spectrum was calculated from non-overlapping windows of about $41\,s$ (i.e. 2048 data points) and then averaged. The spectra at different time intervals are shown in Fig. 2. It is interesting to note the development of a power law spectrum and the shift of the peak of the spectrum towards lower frequencies in time. Both these effects are an evidence of a nonlinear transfer of energy during the wind sea evolution. A power law f^{-4} consistent with the Weak Wave Turbulence theory [37] is also observed.

A representation of the energy spectrum as a function of frequency and direction of propagation was computed with a wavelet directional method [38] from data recorded by the three-gauge array. The directional wave spectra are shown in Fig. 3. Those spectra highlight the fact that energy also spreads over angles, analogously to real ocean waves forced by the wind. Note that the directional distribution is asymmetric in the directional domain due to a non-uniform cross-tank distribution of the wind speed. During the growth phase, energy moves toward lower frequencies, developing a rather narrow banded peak. At the same time, the energy concentrates over a narrower directional band (see righthand panel in Fig. 3).

Using the wave spectra, it is possible to calculate the evolution in time of the significant wave height H_s (i.e. four times the standard deviation of the surface elevation), the peak period and the steepness. The latter is a

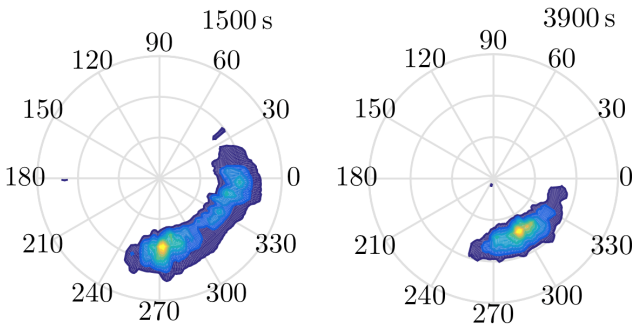

FIG. 3. Example of directional wave spectra. Concentric lines indicates radiant frequency of 5, 10 and 15 rad/s from inside to outside.

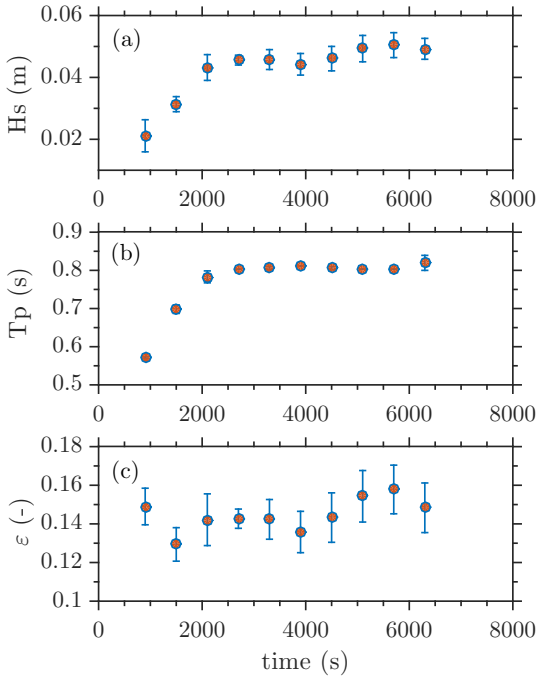

FIG. 4. Temporal variation of the significant wave height H_s (a), peak period T_p (b) and wave steepness ε (c).

measure of the degree of nonlinearity of the system and is defined as $\varepsilon = k_p H_s/2$ with k_p being the wavenumber at the spectral peak. Such quantities are displayed in Fig. 4. We recall that at time $t = 0$ the surface is flat. As the wind starts, waves grow until they reach a quasi-stationary state characterised by a constant H_s of about $0.048\,m$ (after more or less half an hour). In oceanography such condition is usually referred to as "*fully developed condition*". Sporadic wave breaking was observed during the evolution. As observed directly from the spectra (Fig. 2), the peak period also grows monotonically until a stationary state is reached (Fig. 4b). The wave steepness remains steady and normally rather high ($\varepsilon = 0.145$, on average) throughout the experiments (i.e. during both the growing and fully developed stage).

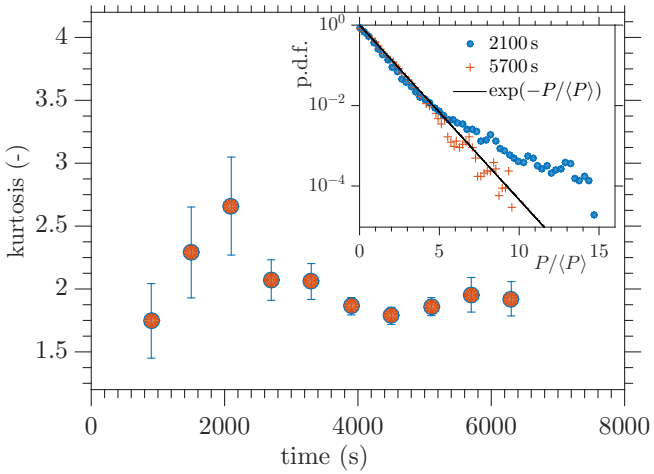

FIG. 5. Temporal evolution of the kurtosis of the wave envelope (main panel) and probability density functions (*p.d.f.*) of the normalised wave intensity $P/\langle P\rangle$ (inset) at the time of maximum kurtosis (2100 s) and at full development (5700 s). The wave intensity is defined as the square modulus of the wave enveloped divided by its mean, The *p.d.f.* for a Gaussian random process, i.e. $-exp(P/\langle P\rangle)$, is shown as reference.

In the physical space, the wave field is characterised by well defined packets, which are consistent with the narrow banded spectral peak; see an example of time series in Fig. 1c. As can be seen from the figure, a rogue wave with height larger than 2.7 times H_s is present in the time series. The fourth-order moment of the probability density function (*p.d.f.*) of the wave envelope (i.e. the kurtosis, a measure of the occurrence of extremes in a record) is calculated to verify whether such a rogue wave is a rare event in a Gaussian population or it belongs to a non-Gaussian distribution (see Fig. 5). Note that the kurtosis is calculated after removing the bound modes, namely the components at frequencies greater than 1.5 and lower than 0.5 times the dominant frequency, which are primarily generated by second-order effects [39]. In doing so, the nonlinear dynamics of free waves remains the only nonlinear mechanisms responsible for the formation of extreme events. If the sea state were a Gaussian random process, the corresponding value of kurtosis would be equal to 2. During the wave growth, however, kurtosis clearly exhibits a monotonic increase until a maximum is reached after 2100 s (main panel in Fig. 5). It is interesting to note that the kurtosis reaches remarkably high values. This strongly non-Gaussian conditions are attained when wave energy focuses both in the frequency and directional domain. The deviation from Gaussianity is substantiated robustly by the heavy tail of the *p.d.f.* of the wave intensity P, i.e. the square modulus of the wave envelope calculated using the Hilbert transform (see the inset in Fig. 5). For longer duration, the kurtosis drops to the value of 2, at which it remains throughout the fully developed stage. Under these circumstances, the tail of the *p.d.f.* of P fits the one expected for a Gaussian random process, i.e. $\exp(-x)$, see inset in Fig. 5. This result

is consistent with numerical simulations of the long-time evolution of the statistical moments of wind seas in [40], where the contribution of free wave nonlinear dynamics to wave statistics is shown to be negligible.

In conclusion, we have presented a laboratory experiment in an annular wind-wave flume to study the statistical properties of wind-generated waves and rogue wave probability. The facility allows the full evolution of the wave field, from its generation to the fully developed stage. As wind starts blowing, an erratic wave field is generated. Rogue waves are detected just before reaching a stationary state. Consequently, strong deviations from Gaussian statistics are observed. We are fully aware that the experimental model is not the ocean. Nonetheless, for the first time, large deviation from Gaussianity have been observed during the development of a wind-forced wave field. To some extent, the condition of infinite fetch modelled in the present experiment exists in the Southern Ocean, where strong winds (the Roaring Forties, Furious Fifties and Screaming Sixties [41]) blow around the Antarctic continent. Waves in the Southern Ocean are indeed regarded to be the fiercest on the planet.

Acknowledgments Experiments were supported by the European Community Framework Programme 7, European High Performance Infrastructures in Turbulence (EuHIT), Contract No. 312778. M.O. acknowledges Dr B. Giulinico and Dr G. Di Cicca for interesting discussions. A. Iafrati is acknowledged for discussions and for providing the wave gauges from INSEAN.

[1] N. Akhmediev, J. Soto-Crespo, and A. Ankiewicz, Phys. Lett. A **373**, 2137 (2009).
[2] K. Dysthe, H. E. Krogstad, and P. Müller, Annu. Rev. Fluid Mech. **40**, 287 (2008).
[3] M. Onorato, S. Residori, U. Bortolozzo, A. Montina, and F. T. Arecchi, Physics Reports **528**, 47 (2013).
[4] M. Erkintalo, Nature Photonics **9**, 560 (2015).
[5] M. Onorato, A. R. Osborne, M. Serio, and L. Cavaleri, Phys. of Fluids **17**, 078101 (2005).
[6] M. Onorato, T. Waseda, A. Toffoli, L. Cavaleri, O. Gramstad, P. A. E. M. Janssen, T. Kinoshita, J. Monbaliu, N. Mori, A. R. Osborne, M. Serio, C. Stansberg, H. Tamura, and K. Trulsen, Phys. Rev. Lett. **102** (2009), 10.1103/PhysRevLett.102.114502.
[7] M. Shats, H. Punzmann, and H. Xia, Phys. Rev. Lett. **104**, 104503 (2010).
[8] A. Chabchoub, N. Hoffmann, and N. Akhmediev, Phys. Rev. Lett. **106**, 204502 (2011).
[9] A. Chabchoub, N. Hoffmann, M. Onorato, and N. Akhmediev, Phys. Rev. X **2**, 011015 (2012).
[10] A. Toffoli, T. Waseda, H. Houtani, T. Kinoshita, K. Collins, D. Proment, and M. Onorato, Phys. Rev. E **87**, 051201 (2013).
[11] D. R. Solli, C. Ropers, P. Koonath, and B. Jalali, Nature **450**, 1054 (2007).
[12] A. Montina, U. Bortolozzo, S. Residori, and F. T. Arecchi, Phys. Rev. Lett. **103**, 173901 (2009).
[13] B. Kibler, J. Fatome, C. Finot, G. Millot, F. Dias, G. Genty, N. Akhmediev, and J. Dudley, Nature Physics **6**, 790 (2010).
[14] B. Kibler, A. Chabchoub, A. Gelash, N. Akhmediev, and V. E. Zakharov, Phys. Rev. X **5**, 041026 (2015).
[15] P. Walczak, S. Randoux, and P. Suret, Phys. Rev. Lett. **114**, 143903 (2015).
[16] N. Akhmediev, B. Kibler, F. Baronio, M. Belić, W.-P. Zhong, Y. Zhang, W. Chang, J. M. Soto-Crespo, P. Vouzas, P. Grelu, *et al.*, Journal of Optics **18**, 063001 (2016).
[17] J. M. Dudley, F. Dias, M. Erkintalo, and G. Genty, Nature Photonics **8**, 755 (2014).
[18] A. N. Ganshin, V. B. Efimov, G. V. Kolmakov, L. Mezhov-Deglin, and P. V. E. McClintock, Phys. Rev. Lett. **101**, 065303 (2008).
[19] H. Bailung, S. K. Sharma, and Y. Nakamura, Phys. Rev. Lett. **107**, 255005 (2011).
[20] Y.-Y. Tsai, J.-Y. Tsai, and I. Lin, Nature Physics (2016).
[21] C. Kharif, E. Pelinovsky, and A. Slunyaev, *Rogue Waves in the Ocean*, Advances in Geophysical and Environmental Mechanics and Mathematics (Springer, Berlin, 2009) p. 216.
[22] C. Kharif and E. Pelinovsky, Eur. J. Mech. B/Fluids **22**, 603 (2003).
[23] A. N. Pisarchik, R. Jaimes-Reátegui, R. Sevilla-Escoboza, G. Huerta-Cuellar, and M. Taki, Phys. Rev. Lett. **107**, 274101 (2011).
[24] B. S. White and B. Fornberg, Journal of fluid mechanics **355**, 113 (1998).
[25] M. G. Brown, Wave Motion **33**, 117 (2001).
[26] E. Heller, L. Kaplan, and A. Dahlen, Journal of Geophysical Research: Oceans **113** (2008).
[27] V. E. Zakharov and L. A. Ostrovsky, Physica D: Nonlinear Phenomena **238**, 540 (2009).
[28] N. Akhmediev, V. Eleonskii, and N. Kulagin, Theor. Math. Phys. **72**, 809 (1987).
[29] M. Onorato, A. Osborne, M. Serio, and S. Bertone, Phys. Rev. Lett. **86**, 5831 (2001).
[30] P. A. E. M. Janssen, J. Phys. Ocean. **33**, 863 (2003).
[31] M. Onorato, A. Osborne, M. Serio, L. Cavaleri, C. Brandini, and C. Stansberg, Europ. J. Mech. B/Fluids **25**, 586 (2006).
[32] G. J. Komen, S. Hasselmann, and K. Hasselmann, J. Phys. Oceanogr. **14**, 1271 (1984).
[33] N. E. Huang and S. R. Long, Journal of Fluid Mechanics **101**, 179 (1980).
[34] A. Zavadsky, D. Liberzon, and L. Shemer, J. Phys. Oceanogra. **43**, 65 (2013).
[35] G. Caulliez and C.-A. Guérin, J. Geophys. Res. **117** (2012).
[36] I. R. Young, *Wind generated ocean waves*, Vol. 2 (Elsevier, 1999) p. 288.
[37] V. E. Zakharov and N. N. Filonenko, in *Soviet Physics Doklady*, Vol. 11 (1967) p. 881.
[38] M. A. Donelan, W. M. Drennan, and A. K. Magnusson, J. Phys. Oceanogr. **26**, 1901 (1996).
[39] M. Longuet-Higgins, J. Fluid Mech. **17**, 459 (1963).

[40] S. Y. Annenkov and V. Shrira, Geophys. Res. Lett. **36** (2009).

[41] D. Lundy, *Godforsaken sea: racing the world's most dangerous waters* (Vintage Canada, 2010).